

**UNCLASSIFIED**

**DAI 14880**

**Armed Services Technical Information Agency**

Reproduced by

**DOCUMENT SERVICE CENTER**

**KNOTT BUILDING, DAYTON, 2, OHIO**

This document is the property of the United States Government. It is furnished for the duration of the contract and shall be returned when no longer required, or upon recall by ASTIA to the following address: Armed Services Technical Information Agency, Document Service Center, Knott Building, Dayton 2, Ohio.

NOTICE: WHEN GOVERNMENT OR OTHER DRAWINGS, SPECIFICATIONS OR OTHER DATA ARE FURNISHED FOR ANY PURPOSE OTHER THAN IN CONNECTION WITH A DEFINITELY IDENTIFIED GOVERNMENT PROCUREMENT OPERATION, THE U. S. GOVERNMENT THEREBY ASSUMES NO LIABILITY, NOR ANY OBLIGATION WHATSOEVER; AND THE FACT THAT THE GOVERNMENT MAY HAVE FORMULATED, FURNISHED, OR IN ANY WAY SUPPLIED SUCH DRAWINGS, SPECIFICATIONS, OR OTHER DATA IS NOT TO BE REGARDED BY ANY PERSON OR CORPORATION, OR CONVEYING ANY RIGHTS OR PERMISSION TO MAKE, REPRODUCE, OR SELL ANY PATENTED INVENTION THAT MAY IN ANY WAY BE RELATED TO THE DRAWINGS, SPECIFICATIONS, OR OTHER DATA.

**UNCLASSIFIED**

**Best  
Available  
Copy**

58277/01  
NO 14 380

# BRFLFC

REPORT No. 988

JULY 1956

## Air Blast Measurements About Explosive Charges At Side-On And Normal Incidence

A. J. HOFFMAN  
S. N. MILLS, JR.

DEPARTMENT OF THE ARMY PROJECT No. D603-04-002  
AND 53-05-016

ORDNANCE RESEARCH AND DEVELOPMENT PROJECT No. TB3-011  
AND TB3-0239

BALLISTIC RESEARCH LABORATORIES



ABERDEEN PROVING GROUND, MARYLAND

BALLISTIC RESEARCH LABORATORIES

REPORT NO. 988

JULY 1, 1956

AIR BLAST MEASUREMENTS ABOUT EXPLOSIVE CHARGES AT  
SIDE-ON AND NORMAL INCIDENCE

A. J. Hoffman

C. N. Mills, Jr.

Department of the Army Project No. 5805-04-002 and 58-05-016  
Ordnance Research and Development Project No. TB3-0112 and TB3-0238

ABERDEEN PROVING GROUND, MARYLAND

TABLE OF CONTENTS

	PAGE
ABSTRACT. . . . .	3
INTRODUCTION. . . . .	5
TEST SET UP . . . . .	6
EXPERIMENTAL PROCEDURE. . . . .	9
COMPUTATIONAL PROCEDURE . . . . .	11
RESULTS . . . . .	14
DISCUSSION. . . . .	19
FUTURE WORK . . . . .	22
REFERENCES . . . . .	25
APPENDIX I: Description and Utility of a "Face-On" Pressure Gage. . . . .	27
APPENDIX II: Description of "Side-On" Gage . . . . .	31
APPENDIX III: Table of Peak Pressures, Impulses and Durations . . . . .	33

BALLISTIC RESEARCH LABORATORIES

REPORT NO. 988

AJHoffman/SNMills/rf  
Aberdeen Proving Ground, Md.  
May 1956

AIR BLAST MEASUREMENTS ABOUT EXPLOSIVE CHARGES AT  
SIDE-ON AND NORMAL INCIDENCE

ABSTRACT

Measurements of air blast peak pressures, positive impulses, and positive durations for both side-on and normal incidence from bare 50/50 spherical pentolite charges are presented. The explosive weight ranged from 1/2 to 8 pounds, the scaled distance from 1.48 to 14.81 ft/lb<sup>1/3</sup>. Results of two hundred and sixty-nine test firings are tabulated and presented graphically. A description is given of the piezoelectric gage developed to measure the blast in the normally incident waves.

## INTRODUCTION

Before the response of a structure to air blast can be predicted, the spatial and temporal loading must be known. Two limiting cases of the blast loading from an explosive charge are (1) the free expansion of the shock wave into undisturbed air (called "side-on") and (2) the reflection at normal incidence of the shock wave from an infinite, rigid wall (called "face-on"). Neither case applies directly for many target structures of military interest, such as aircraft or buildings, because of diffraction. However, peak pressures and impulses\* for (1) and (2) represent, in general, lower and upper bounds respectively to the actual loading, and thus may establish limits for calculations of structural response.

Theoretical relations have been advanced for the dependence of side-on peak pressure and impulse on distance.<sup>1,2,3\*\*</sup> Moreover, the relation between side-on and face-on peak pressure is known theoretically as a function of the velocity of propagation of the shock front.<sup>4</sup> On the other hand, theories of face-on impulse are limited to relatively weak shocks.<sup>5,6</sup> Experiments to check these theoretical relations have been extensive,<sup>7</sup> but for the case of side-on impulse have been limited to scaled distances greater than 4 or 5  $\text{m}/\text{lb}^{1/3}$ . There are practically no data of face-on impulse, especially close to the surface of explosive charges where shocks are quite intense. Since knowledge of the impulse, both side-on and face-on, is very necessary for the prediction of the response of structures to air blast loading, it was decided to carry out a series of experiments to make impulse measurements over an extensive range of scaled distances, concentrating especially at small distances.

---

\* Defined as the positive area under the pressure-time history,  
 $I = \int_0^t P(t)dt$ , where  $P$  is the excess pressure and  $t$  is equal to the positive duration

\*\* Numbers refer to reference on page 25.

The present study extends face-on impulse measurements closer to the explosive charge surface than were obtained in a preliminary study reported in Ballistic Research Laboratory Technical Note 786.<sup>8</sup> With the development of a suitable gage it was possible to make measurements as close as 1.5 ft/lb.<sup>1/3</sup> where the face-on pressure is about 3200 pounds per square inch. The gage development required lengthy experimentation to minimize the effects of accelerometer action resulting from the transfer of momentum to the gage (transducer) by the normally incident shock wave. These accelerometer effects were found to be reduced satisfactorily when the transducer was mounted as an integral part of an extremely massive, reinforced concrete wall. The gage that was found satisfactory and used for these experiments is described in Appendix I.

With an adequate combination of transducer and reflecting surface, measurements were taken using explosive charges of bare 50/50 spherical pentolite of 1/2-, 1-, 2- and 6-pounds. These explosive weights provided an adequate check on scaling laws<sup>9</sup> and permitted measurements over a greater range of pressures than could be achieved with any one charge weight.

#### TEST SET-UP

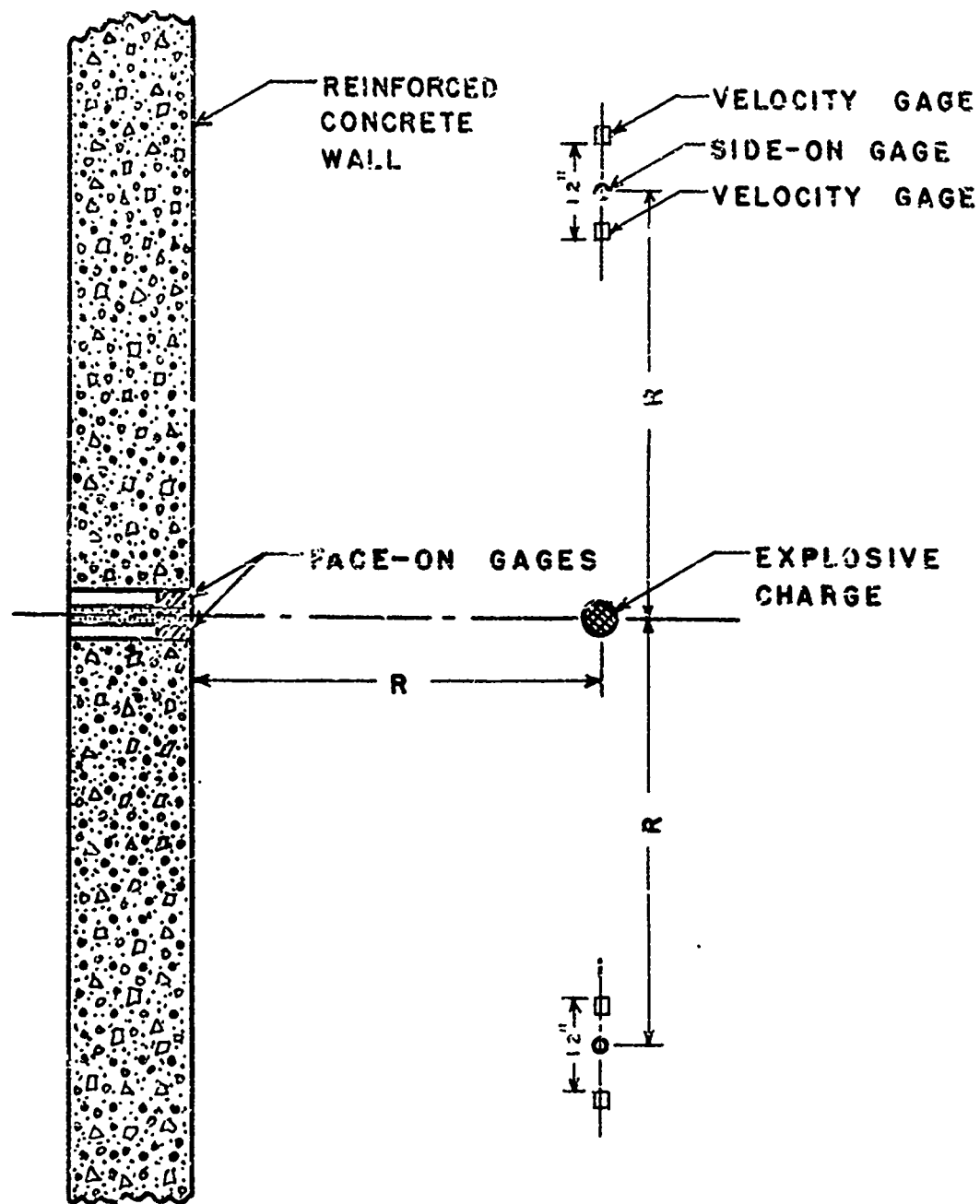
The experimental test facilities used for obtaining the blast measurements consisted of massive reflecting surfaces of sufficient size to prevent diffraction of the blast wave before the completion of the positive loading phase. Two such surfaces were employed during the course of the tests, one the wall of a chamber made of two-foot thick reinforced concrete, and the other a 10 ft. x 10 ft. x 1 ft. concrete slab poured on the ground surface. One and one-half inch diameter mounting pipes, with threaded sleeves, were inserted in each of these surfaces to receive and retain the face-on transducer housings flush with the surface. Such mounting permitted the surface of the sensing element of the gage to become essentially an element of the reflecting surface. See Figure 1.

On a line perpendicular to the reflecting surface through the center of an array of face-on gages, as shown in Figure 2, a bare 50/50

FACE-ON GAGES FLUSH-MOUNTED  
IN  
CONCRETE REFLECTING SURFACE



FIGURE 1



ARRANGEMENT OF GAGES ABOUT  
EXPLOSIVE CHARGE

FIGURE 2

spherical pertolite charge was suspended from an overhead support. In a plane parallel to the reflecting surface through the explosive charge, two positions of side-on air blast gages (see Appendix II) were placed at the height of the charge center. These positions were oriented 180 degrees apart with each gage pointing directly at the center of the explosive. The resulting configuration was that of both side-on and face-on gages lying on points of a circle about the explosive charge as center. Each of the side-on gages was spanned by two piezoelectric "velocity" gages such that they were at the midpoint of the velocity interval. A "velocity" gage merely records time of arrival of the shock front.

The signals from all gages were transmitted through RG62-U coaxial cables having a capacity of 13.5 micro-micro farads per foot to appropriate recording equipment. Pressure-time histories of the blast waves were photographically recorded from cathode ray oscillographic traces and the times of arrival of the shock wave were indicated on electronic counter chronographs.

Meteorological equipment was also provided at the test site for measuring the wind direction and velocity, and ambient atmospheric temperature and barometric pressure.

#### EXPERIMENTAL PROCEDURE

Prior to making each test firing the explosive was weighed with an analytical balance. The individual weights within a given group of nominal weight were found to differ negligibly from each other since each lot of charges was cast in precision molds. Sample measurements of the density of the explosive were taken for both 1-pound and 8-pound charge weights. Ten spherical charges of each weight were selected at random and values of densities determined. The average density of the 1-pound and 8-pound spheres was found to be 1.588 and 1.612 respectively. (These values are the approximate limits for all of the charge weights used and the density for all explosive weights over the range of the experiments probably differ negligibly from the average of these two.)

Each test charge was suspended from an overhead support and so guyed into position that the radial distances from the charge center to all waveform gages (face-on and side-on) were equal. The interval between the two velocity gages at each position was measured accurately with a jig which assured proper spacing both vertically and horizontally about the side-on gage stationed at the midpoint. Each explosive charge was initiated at its center with a Corps of Engineers special electric detonator to assure reproducible initiation of all charges over the range of weights used. The detonators and the electrical leads were oriented in such a manner that any metal fragments resulting from the detonation would be directed away from the gages.

Before a group of explosives was fired, all gages and connecting cables were checked for continuity and proper impedance. A gage or line was replaced wherever its impedance dropped below 1000 megohms because the excess leakage of electrical charge that would thereby be caused could lead to inaccurate measurements of duration. The individual firings were conducted from an automatic sequence timer which initiated the detonation of the explosive charge, started the high speed recording cameras, and intensified the sweep of the oscillographic traces. Measurements of ambient temperature, atmospheric pressure and the wind direction and velocity in the vicinity of the tests were obtained as near to the time of firing as possible. Immediately after each round the shock wave arrival times were recorded and irregularities noted. Film records of the pressure-time histories were processed promptly so that any discrepancies arising in the system might be detected and corrected without an appreciable loss of data. Since the blast parameters (excess pressure, positive impulse and positive duration) were desired over as great a range of scaled distances\* as practicable,

---

\* Scaled distance,  $z$ , is equal to  $R/W^{1/3}$  where  $R$  is the distance to the charge center and  $W$  the weight of explosive.

identical firings were repeated at each of many different scaled distance values until reliable statistical averages were obtained.

#### COMPUTATIONAL PROCEDURE

##### I. Side-on Pressure

Measurement of the transit time of the blast wave over a fixed distance interval between a pair of velocity gages yields an average velocity over the interval. This velocity has been shown to be equal to the velocity at the interval midpoint<sup>10</sup> where side-on gages are located. A mean value of the shock velocity for calculating the excess shock pressure was obtained by averaging the measured transit times for the two positions of velocity gages.

Excess side-on pressures were obtained from the Rankine-Hugoniot condition

$$\frac{P_S}{P_O} = \frac{2\gamma}{\gamma + 1} \left[ \frac{V^2}{C^2} - 1 \right] \quad (1)$$

where

- $P_S$  = side-on excess pressure, psi
- $P_O$  = Ambient atmospheric pressure, psi
- $V$  = shock velocity in still air, ft/sec
- $C$  = sound velocity in air ahead of shock, ft/sec
- $\gamma$  = ratio of specific heats (equal to 1.4 for air)

This relation was used over the range of pressures for which  $\gamma$  was essentially equal to 1.4. For pressures higher than 20 atm.  $\gamma$  is no longer constant since air does not behave as an ideal gas. For these higher pressures the specific heat at constant volume,  $C_v$ , was assumed to be a linear function of temperature and the side-on pressure was obtained from the velocity of propagation using data prepared by Doering and Burkhardt.<sup>3</sup>

## II. Face-On Pressure

Assuming the shock wave to be spherically symmetric,\* inferences of the face-on pressure at the reflecting surface, where transit time measurements of the shock wave could not be taken, were made from a knowledge of the side-on pressure using the relation<sup>4</sup>

$$\frac{P_r}{P_s} = 2 + \frac{6y}{y+1}$$

where  $P_r$  = face-on excess pressure, psi  
 $y = P_s/P_o$

In this expression,  $P_s$  is the excess side-on pressure computed from equation (1) using an average of the shock velocities at the two side-on positions.<sup>\*\*</sup> This relation also fails for side-on pressures above 20 atmospheres. Therefore, face-on pressures in the high pressure region were obtained by again using an analysis due to Doering and Burkhardt.<sup>3</sup>

---

\* This assumption appears valid since spherical charges were used and measurements by velocity gages, orientated 180 degrees apart, indicated symmetry except for small perturbations.

\*\* If the blast wave had spherical symmetry, except for small perturbations, this value of  $P_s$  computed from the average value of shock velocity would more likely yield the side-on pressure incident on the reflecting surface than would the value of  $P_s$  calculated at either position.

### III. Gage Constants

With excess pressures known from the velocity measurements, gage sensitivities for both side-on and face-on gages were computed from the formula

$$KA = \frac{H}{S} \times \frac{Q}{P}$$

where

KA = gage sensitivity, micro-microcoulombs/psi

H = height of initial peak of pressure-time history on a record

S = average voltage calibration step size on a record

Q = calibration charge, micro-microcoulombs

P = excess pressure, psi

Heights of H and S were measured on the same arbitrary scale from the individual record.

Calculated values of the individual gage constants appeared to be somewhat erratic because of inability to determine accurately the magnitude of the initial peak. These variations were most pronounced with high pressure, short duration pulses. Since static calibrations\* of several gages showed the gage sensitivity to be linear over a range of pressures from 100 to 10,000 pounds per square inch, a mean of the KA was assumed over all firings to which the gage was subjected.

---

\* A static calibration consists of subjecting a gage to a precisely known pressure and recording the output on a galvanometer when the load is suddenly released. This calibration, while indicating linearity, does not yield a KA necessarily equal to the KA obtained in field firing.

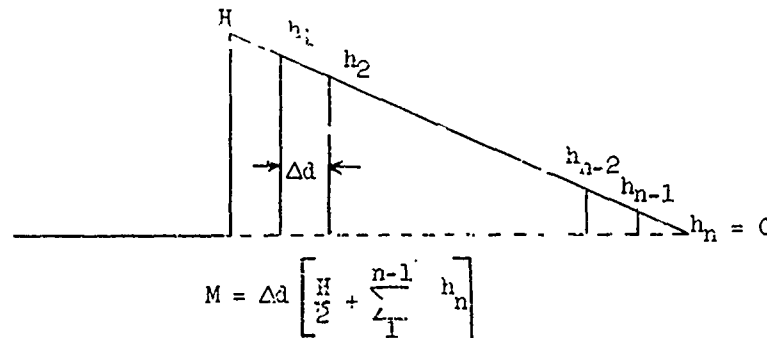
This mean value was then used to compute the positive impulse of each round for which the gage was used.

#### IV. Positive Impulses

Positive impulses were obtained from the formula  $I = \frac{M \times Q}{KA \times U \times S}$

where  $I$  = impulse, p i-ms.  
 $M$  = area under the positive phase  
 $U$  = time scale factor, scale units/ms.

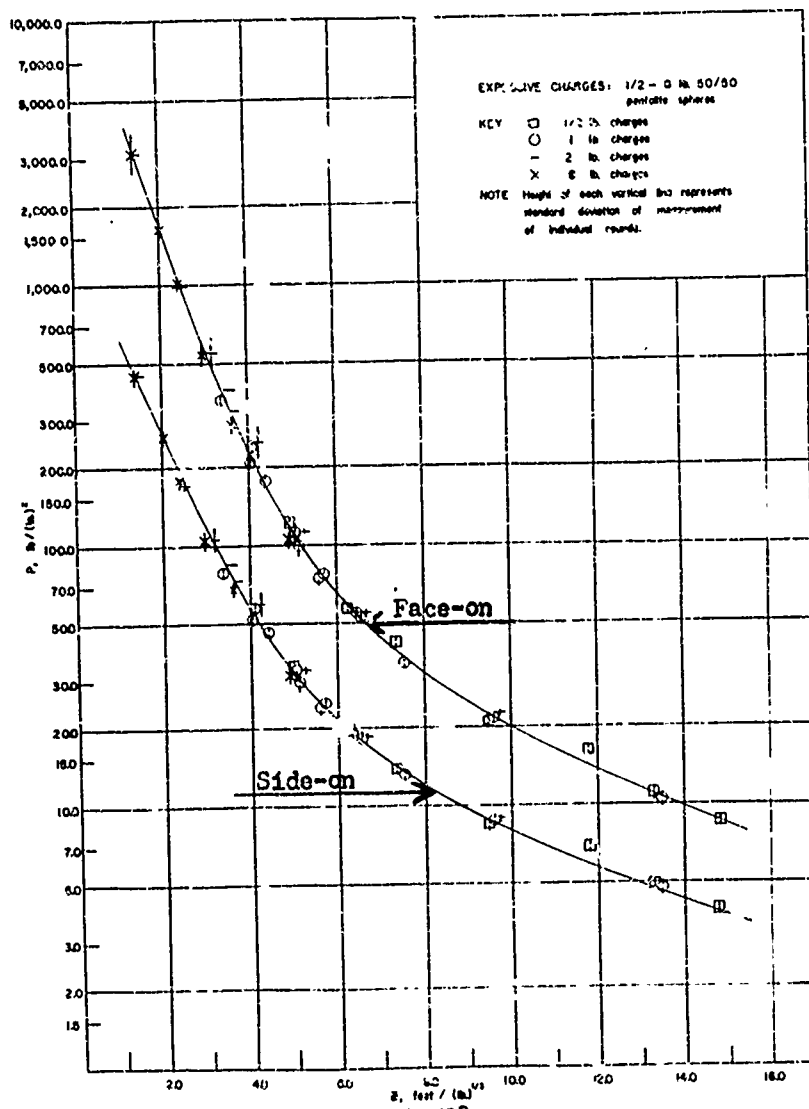
The area  $M$  was computed by the trapezoidal rule from ordinates measured at small equal intervals on the film records as shown below (all measurements to the same scale as  $S$ ).



The films were read on precision film readers by the Analytical Laboratory, Development and Proof Services, and the data obtained were tabulated and recorded on IBM cards. From these tabulated data, the Computing Laboratory of BRL computed the impulses.

#### RESULTS

Excess pressures, positive impulses and positive durations over a range of scaled distances from 1.48 to 14.81 ft/lb.<sup>1/3</sup> and a range of explosive weights from 1/2 to 8 pounds are presented graphically in figures 3, 4, and 5 respectively. These data represent 269 firings for which individual values of the last parameters, and also average values for a given group are reported in Appendix III. Typical records of side-on and face on pressure-time histories are presented in Figure 6. These parameters were found to scale according to the dimensional laws proposed by Sachs<sup>9</sup>,



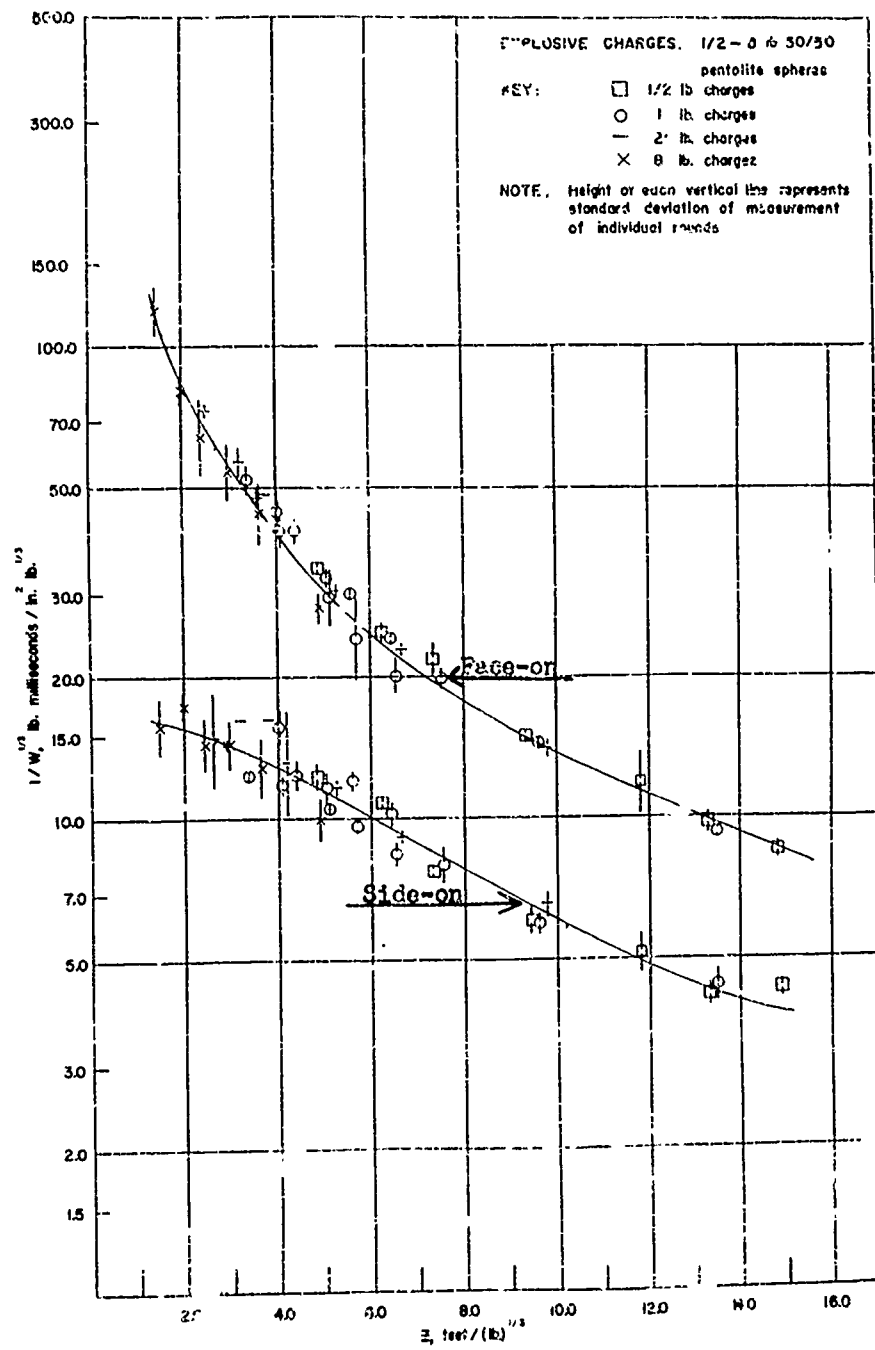


FIGURE 1  
FACE ON AND SIDE ON  
SCALED IMPULSE VS. SCALED DISTANCE

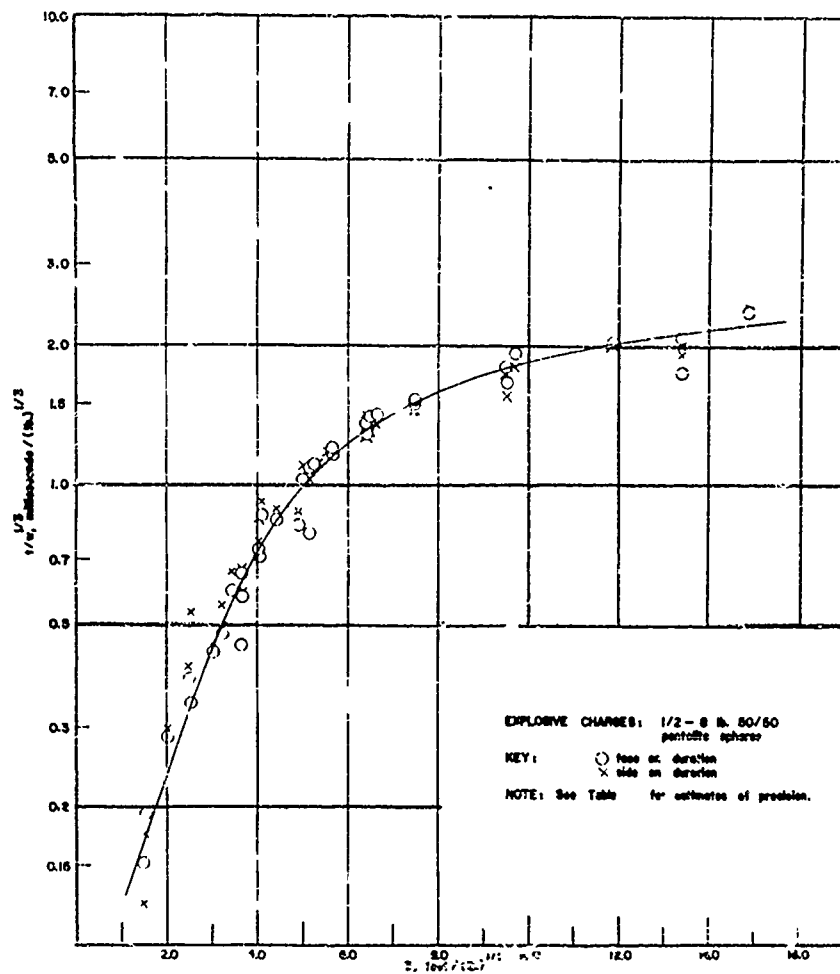
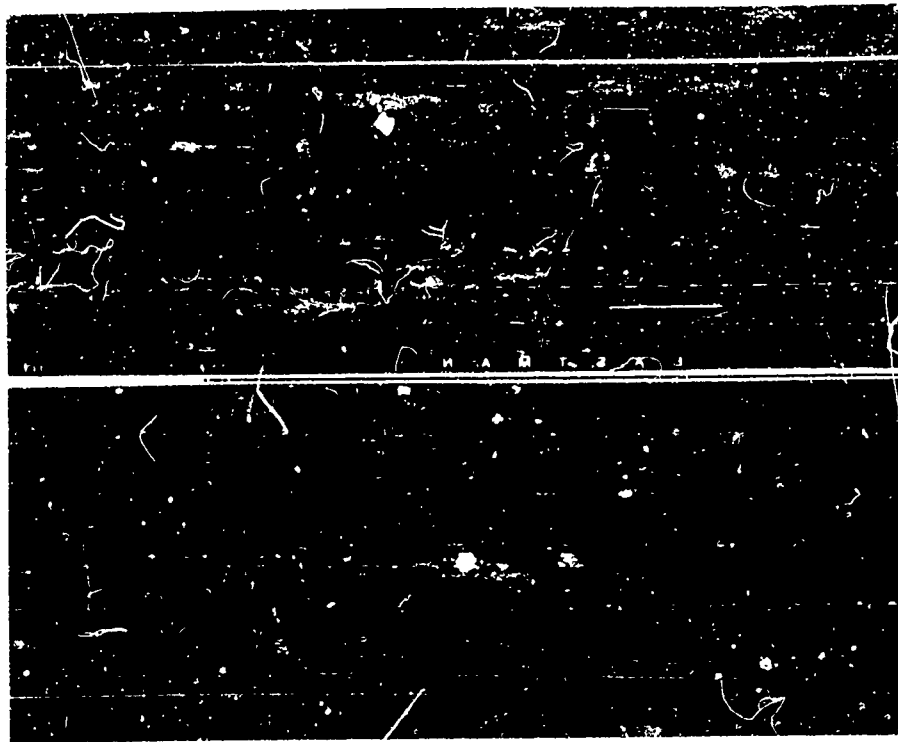


FIGURE 5  
FACE ON AND SIDE ON SCALED DURATION vs. SCALED DISTANCE

PRESSURE-TIME HISTORIES FROM 50/50 PENTOLITE SPHERES

ROUND 105



face-on  
face-on  
side-on  
side-on

face-on  
face-on  
side-on  
side-on

ROUND 112

FIGURE 6

and the different explosive weights used are presented on scaled curves for both reflected and side-on incidence. The durations of the reflected and side-on blast waves, however, were found to be statistically equal within the range of experiments and are combined into a single scaled duration curve.

#### DISCUSSION

The range of scaled distances over which data were taken is the region of great interest for structural damage from high explosive charges. However, the exact limits of the range chosen were dictated by test conditions. It was found that in the high pressure region the rapid fall-off and short duration of the pressure-time histories made accurate readings of areas under the curves difficult. In addition, the quality of the records deteriorated as the gages were placed closer and closer to the explosive charge. In light of these facts, it was decided that data taken at scaled distance values less than about 1.5 would be questionable, and high pressure tests were accordingly discontinued at 1.48. The upper limit of scaled distance was taken at approximately 15 because it had been found in many test firings against a variety of target structures that scaled distances greater than 15 are out of the damage region for explosive weights less than 1000 pounds. Threshold damage to military targets tends to be a function of only peak pressure for weights beyond several thousand pounds.

A measure of the precision of the measurements may be seen in Figures 3, 4, and 5, and Appendix III, where the standard deviations for each set of firings are given. Values of side-on pressure and impulse presented are in good agreement with the average curves of data taken previously by these Laboratories. However, side-on impulses are somewhat at variance with the predictions of Kirkwood and Brinkley as shown in Figure 7. The question of correcting all impulse measurements to allow for differences in ambient temperature was considered, but investigation showed that the extremes of the temperature range could account for less than a 5 percent

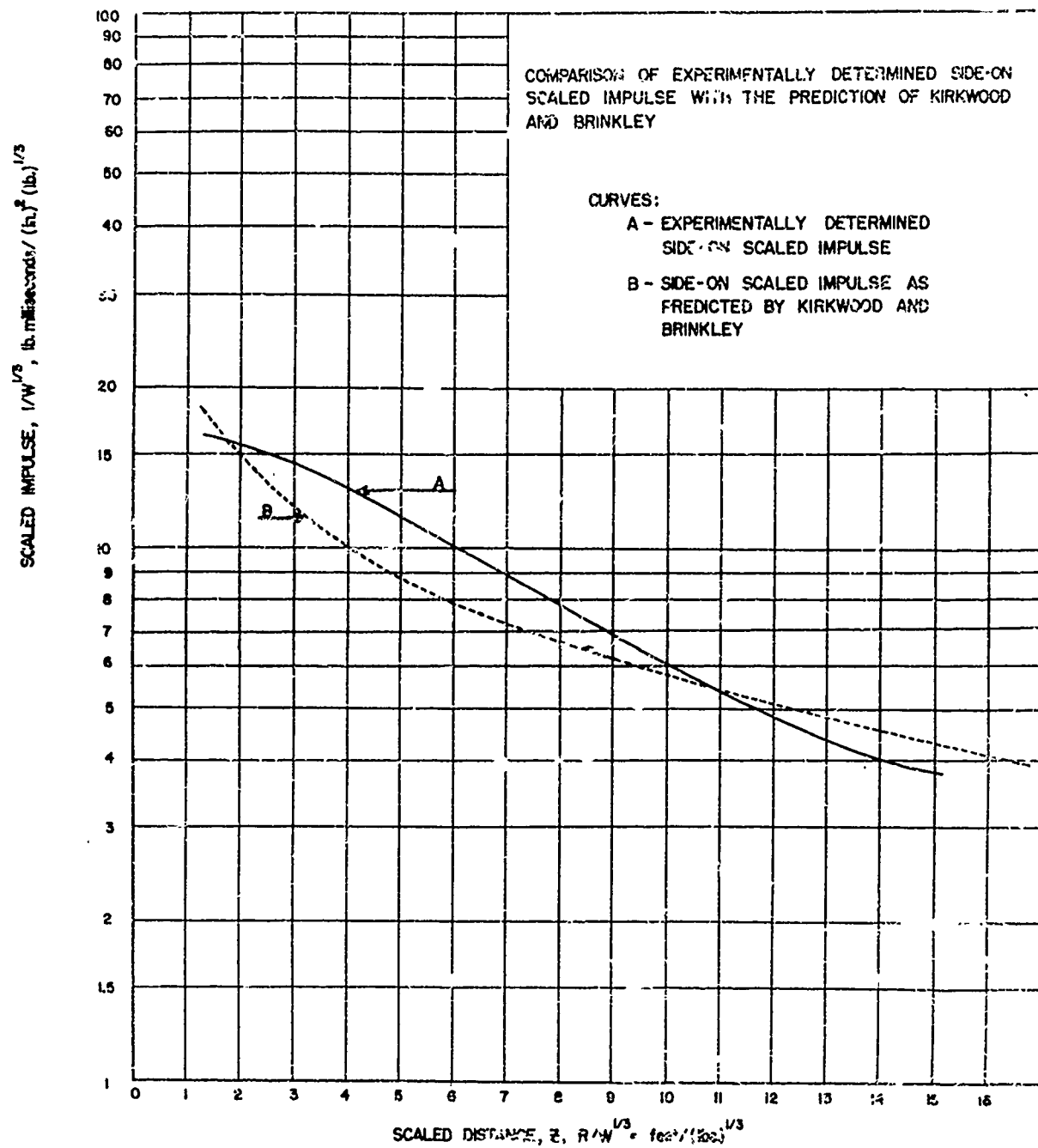


FIGURE 7

variation in impulse. Since the standard deviations of the impulse measurements averaged approximately 10 percent, the temperature correction was not included.

Fitting analytical expressions to the data was given careful consideration. It was desired to fit the data accurately, but physical considerations made using the method of least squares undesirable. An objection to finding analytic expressions for the data is that no reliable extension beyond the range of measurement could be made from these expressions. This follows from the fact that the range of measurement extends just into the pressure region where the ideal gas assumption for air breaks down. Therefore, no reliable extrapolation of the data could be made. Indeed, Kirkwood and Brinkley<sup>2</sup> have predicted that the side-on impulse curve goes through a maximum at a scaled distance of 1.00, and an analytic fit to the data could never be expected to show a maximum outside the range of measurements. Therefore a method of centroids was used to plot curves through the data. Groups of points were chosen, and the weighted average of the coordinates was calculated. These weighted average points described smooth curves, from which reliable values of the blast parameters could be obtained.

It is believed that measurements of face-on impulse and face-on duration at scaled distances less than 5 are being presented for the first time. Face-on impulses from a scaled distance of 5 to 15 are in agreement with results of preliminary firings presented previously.<sup>8</sup>

Since the face-on duration equals the side-on duration within experimental error, it seems logical to attempt to relate the face-on and side-on impulse analytically by using a relation between face-on and side-on pressure. Makino and Shear<sup>11</sup> have attempted to fit the experimentally determined face-on impulse curve by assuming the normal reflection formula to hold behind as well as at the shock front. With this assumption it is

---

\* Weighted according to the number of observations.

possible to find face-on impulse by integration for any known shape of the side-on pressure-time history. Three cases were chosen by Makino and Shear for comparison with the experimental results:

Case I:  $p_s(t)$  was assumed to decay exponentially with time,

$p_s(t) = P_s e^{-kt}$ , where  $P_s$  is the peak side-on pressure and the constant  $k$  is adjusted to fit known conditions. The normal reflection formula,

$$\text{where } p_r(t) = p_s(t) \left( 2 + \frac{6y}{y+7} \right)$$

$p_r$  = face-on pressure

$y$  =  $p_s(t) / P_0$

$P_0$  = ambient atmospheric pressure

was then integrated to obtain the face-on impulse.

Case II:  $p_s(t)$  was taken to decay linearly with time,  $p_s(t) = P_s(1 - kt)$ , and the face-on impulse again was found by integrating the normal reflection formula.

Case III:  $p_s(t)$  and  $p_r(t)$  were both taken to decay linearly with time.

The curves of reflected scaled impulse as a function of scaled distance for these three cases are shown in comparison with the authors' experimental results as Curves I, II and III in Figure 8. Curve I appears to show the best agreement. This is consistent with work performed at these Laboratories and also other installations which associates an exponential shape with the side-on pressure-time history.

#### FUTURE WORK

It is desired to obtain a check on the accuracy of reflected impulse measurements by a method independent of piezoelectric gages. Experimentation is presently in progress to adapt strain gages on rods and strain gage transducers to impulse measurements. Still another technique is in progress whereby impulse is inferred from the momentum-impulse theorem by measuring the initial velocity imparted to a given mass by the impulsive blast wave loading. It is hoped with the later technique to

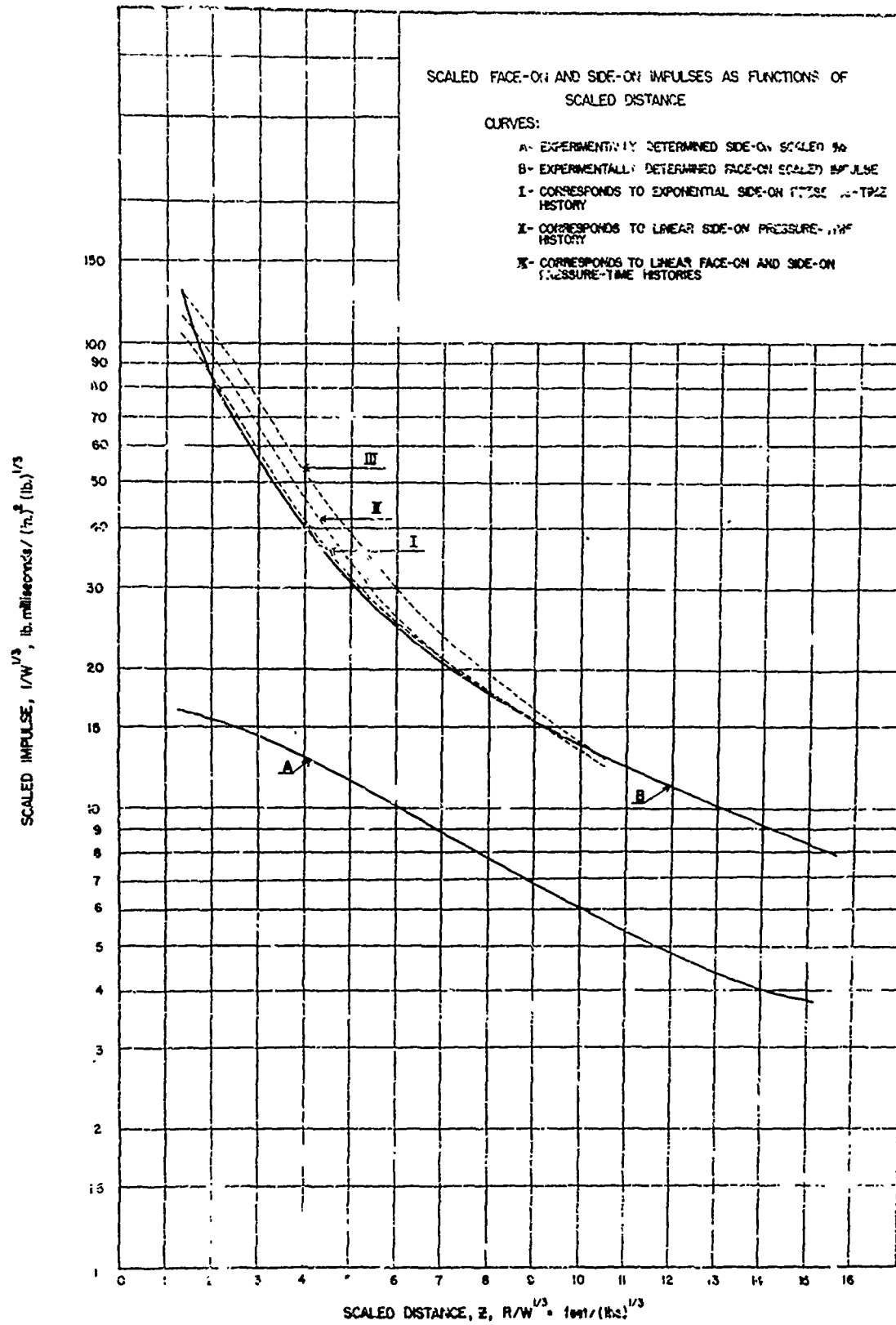


FIGURE 8 25.

extend measurements of reflected impulse to shorter scaled distance values where it is believed that impulse loading alone is a criterion for damage to many structures.

It is also hoped that measurements of excess peak pressure, positive impulse and positive duration can be made at different altitudes to provide adequate checks on Sach's altitude scaling laws. With such measurements, better estimates of the letdown envelopes around aircraft and missiles for blast type warheads and correlation of internal blast damage tests with blast measurements may be possible.

*A. J. Hoffman*  
A. J. HOFFMAN

*S. N. Mills Jr.*  
S. N. MILLS, JR.

#### REFERENCES

1. Courant, R., and Friedrichs, K. O., Supersonic Flow and Shock Waves. Interscience Publishers, Inc., New York, 1948. pp. 149, 153.
  2. Kirkwood, J. G. and Brinkley, S. R., "Theory of the Propagation of Shock Waves from Explosive Sources in Air and Water," NDRC Report No. A-318, March, 1945.
  3. Doering, W. and Burkhardt, G., Contributions to the Theory of Detonation (Translation from German prepared by Brown University) Technical Report No. F-TS-1227-1A (GDAM A 9-F-46), Headquarters, Air Materiel Command, Wright-Patterson Air Force Base, Dayton, Ohio, May, 1949.
  4. Lampson, C. W., "Résumé of the Theory of Plane Shock and Adiabatic Waves with Application to the Theory of the Shock Tube," BRL Technical Note No. 139, Aberdeen Proving Ground, Maryland, March 1950, p. 26.
  5. Chandrasekhar, S., "Normal Reflection of a Blast Wave," BRL Report No. 439, Aberdeen Proving Ground, Maryland, December, 1943.
  6. Finkelstein, R., "Normal Reflection of Shock Waves," Explosion Research Report No. 6, Navy Department, Bureau of Ordnance, Washington, D. C., August, 1944.
  7. Stoner, R. G., and Bleakney, W., "The Attenuation of Spherical Shock Waves in Air," Journal of Applied Physics, Vol. 19, No. 7, pp 670-678, July, 1948.
- Dewey, J. and Sperrazza, J., "The Effects of Atmospheric Pressure and Temperature on Air Shock," BRL Report No. 721, Aberdeen Proving Ground, Maryland, May, 1950.
- Curtis, W., "Free Air Blast Measurements on Spherical Pentolite," BRL Memorandum Report No. 544, Aberdeen Proving Ground, Maryland, July 1951.
- Sultanoff, M. and McVey, G., "Shock Pressure at and Close to the Surface of Spherical Pentolite Charges Inferred from Optical Measurements," BRL Report No. 917, Aberdeen Proving Ground, Maryland, August, 1954.
8. Goldstein, H. and Hoffman, A., "Preliminary Face-On Air Blast Measurements," BRL Technical Note No. 788, Aberdeen Proving Ground, Maryland, April, 1953.
  9. Sachs, R. G., "The Dependence of Blast on Ambient Pressure and Temperature," BRL Report No. 466, Aberdeen Proving Ground, Maryland, May 1944.
  10. Cooney, I. M. and Sperrazza, J., "The Position at Which the Velocity of a Blast Wave Equals the Average Velocity over an Interval," BRL Memorandum Report No. 541, Aberdeen Proving Ground, Maryland, May, 1951.

REFERENCES (Continued)

11. Makino, R. C. and Shear, R. E., "Estimation of Normal Reflected Impulse of Blast Waves," BRL Technical Note No. 1010, Aberdeen Proving Ground, Maryland, May, 1955.

## APPENDIX I

### Description and Utility of a "Face-on" Piezoelectric Gage

This gage, usually referred to as a "face-on gage," is a piezoelectric transducer used to record the pressure-time history of an air blast wave reflected from the surface of a rigid structure. Essentially, this gage is an element of the reflecting surface and is designed to measure the blast loading impinging on the structure less any structural response.

The sensitive element of the face-on gage consists of two disc-shaped tourmaline crystals, each approximately 0.040 inch thick and 0.75 inch in diameter cemented into a stack together with a copper foil electrode of the same diameter inserted between the positive faces. The negative faces of the crystals are electrically connected through the flap of a second copper foil disc cemented to the lower face of the stack. The entire sensitive element is bonded under pressure to the bottom of a 0.100 inch deep by 1.00 inch diameter cavity located in the threaded end of a brass housing. The electrical charge collected by the positive foil is transmitted by a fine wire through the housing to a coaxial connector on the opposite end while the negative connection is made directly to the gage housing. The clearance between the element and housing is finally filled with a chemically hardened potting compound which, when filed smooth and flat, provides a thin hard surface over the crystals. This construction is relatively invulnerable to high intensity loading except for direct hits from occasional fragments. A schematic drawing of this gage is shown in Figure 9.

Several techniques concerned with measurements of reflected pressures with a piezoelectric gage were revealed through considerable experimentation. It was first discovered that a rigid backing for the crystal stack was necessary to prevent spurious signals resulting from flexure of the crystals under load being superimposed on the record. It was ascertained also that a housing with considerable mass was desirable to prevent excessive gage motion for the duration of the pulse. These characteristics were resolved through use of cylindrical brass housings, approximately 1.5 inches in diameter, and ranging from four to six inches in length.

FACE-ON GAGE

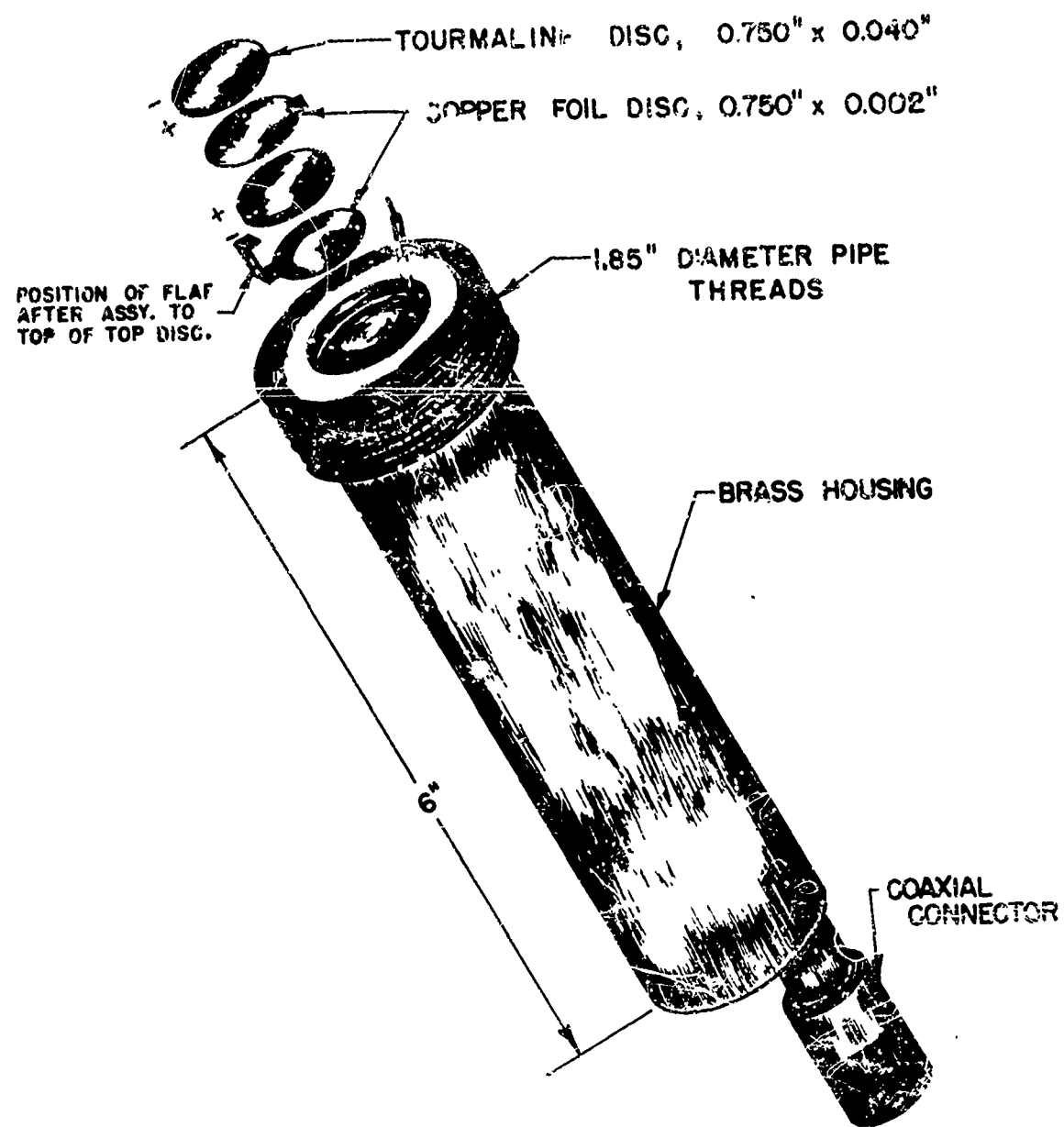


FIGURE 9

APPENDIX I (Continued)

Initially, a flat steel plate was used as a reflecting surface. The pressure-time history of the blast wave was masked by oscillations caused by vibrations of the plate, which were coupled through the gage housing to the sensing element. Attempts to isolate the gage from the reflecting surface resulted in relative motion between the gage and reflector which appeared on the record as an acceleration response due to translation of the gage under the blast load. As a result, an extremely massive reflecting surface was suggested in which these phenomena could not occur. The face-on gage was finally secured into a rigid concrete structure as an element of the surface. Satisfactory reflected pressure-time histories, relatively free from spurious oscillations, were then obtained up to pressure intensities of about 4000 pounds per square inch.

## APPENDIX II

### Description of "Side-On Gage"

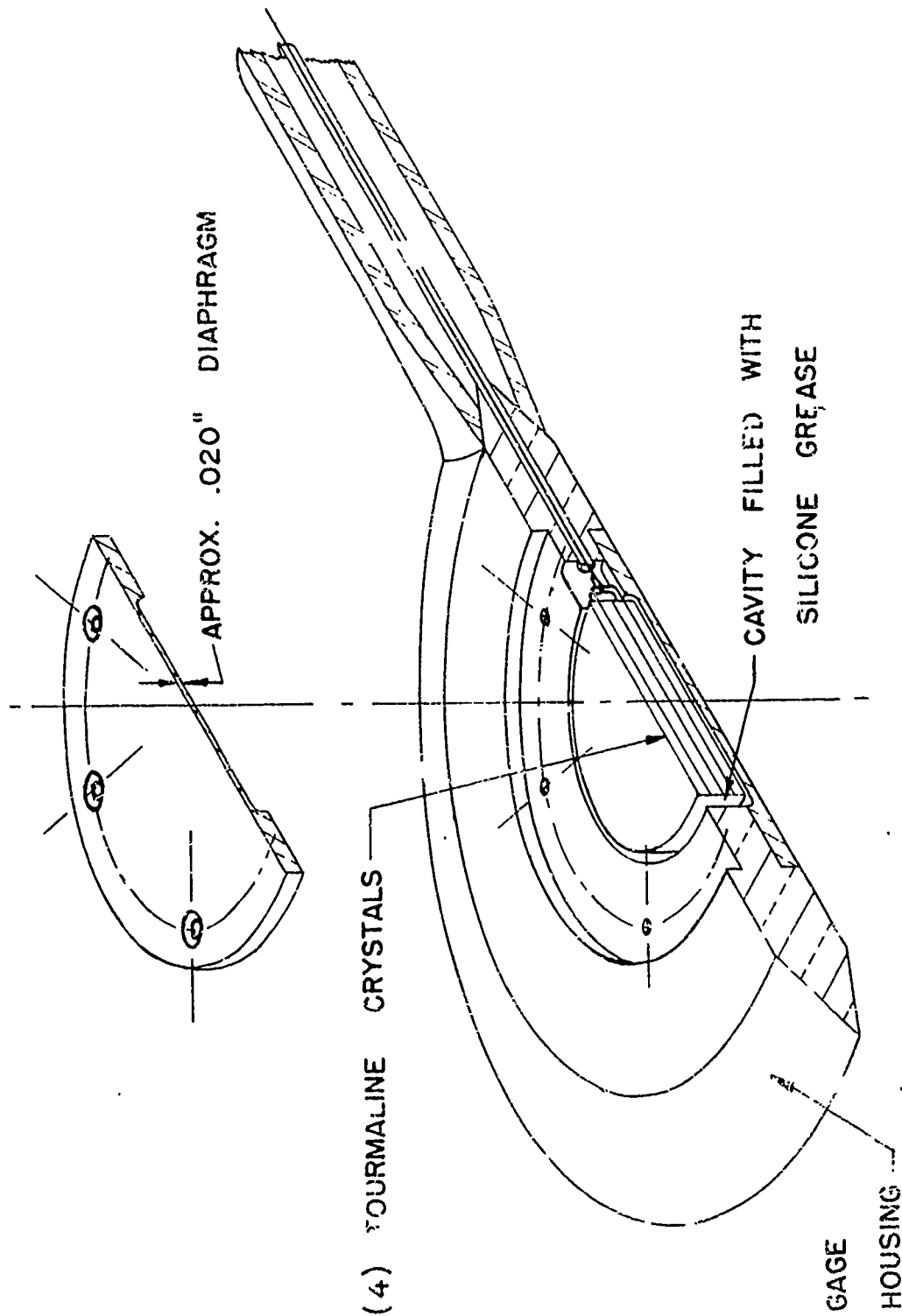
The Stressed Diaphragm BRL Gage is a piezoelectric air blast gage for recording the side-on pressure-time history associated with blast waves. This gage, which in its original form was developed by Mr. Roy Sampson, formerly of BRL, has been used with a great deal of success in small charge (3/8 lb. to 64 lb.) air blast experiments.

The sensitive element of the Stressed Diaphragm BRL Gage is a stack of four wafer shaped tourmaline crystals, approximately .050 inches thick, with silver foil electrodes between crystals to collect the charge. The crystals are usually one inch or one-half inch in diameter but gages have been built in which the diameter of the crystals was as small as one-eighth inch.

The design principle which is believed to be most directly responsible for the success of the S.D.BRL Gage is the preloading of the crystal stack by brass diaphragms approximately .020 inches thick. Interference between the crystal stack and the cavity in the gage housing of from .0005 to .002 inches has been found to give the best results. Silicon grease applied between the faces of the stack and the brass diaphragms as well as in the clearance around the stack is helpful in damping spurious oscillations.

The quality of the workmanship in machining the housing, grinding and polishing the tourmaline crystals, and assembling the crystals into the housing has been found to be of the utmost importance in producing gages which give records of high fidelity. A schematic drawing of this gage is shown in Figure 10.

FIGURE 10



THE STRESSED DIAPHRAGM BRL GAGE

APPENDIX III

TABLE OF PEAK PRESSURES, IMPULSES AND DURATIONS





Pd. No.	Ambient Pressure Psi	Ambient Temp °C	Charge Wt. (lbs)	Scaled Distance ft/lbs <sup>1/3</sup>	Peak Pressure Psi		Impulse of Positive Phase in lb msec/in <sup>2</sup>				Duration of Positive Phase in msec				Average Scaled Impulse		Average Scaled Duration	
					Side-On	Face-On	Pos. 1	Pos. 2	Pos. 3	Pos. 4	Side-On	Pos. 1	Pos. 2	Pos. 3	Pos. 4	Side-On	Face-On	Side-On
59	14.60	15.6	1.050	5.04	34.46	121.08	12.29	32.52	32.37	32.57	32.57	32.57	32.57	32.57	32.57	32.57	32.57	32.57
60	14.60	14.9	1.050	5.04	32.29	111.09	10.29	30.82	30.82	31.33	31.33	31.33	31.33	31.33	31.33	31.33	31.33	31.33
61	14.60	14.2	1.050	5.04	31.20	106.21	11.22	31.51	31.51	32.52	32.52	32.52	32.52	32.52	32.52	32.52	32.52	32.52
62	14.60	12.8	1.050	5.04	31.17	116.32	11.99	31.51	31.51	32.52	32.52	32.52	32.52	32.52	32.52	32.52	32.52	32.52
63	14.62	15.0	1.050	5.04	35.98	122.12	11.94	34.14	34.14	35.25	35.25	35.25	35.25	35.25	35.25	35.25	35.25	35.25
64	14.62	17.2	1.050	5.04	30.48	102.91	12.14	31.64	31.64	31.69	31.69	31.69	31.69	31.69	31.69	31.69	31.69	31.69
Av					31.33	115.70	11.85	32.91	32.91	32.91	32.91	32.91	32.91	32.91	32.91	32.91	32.91	32.91
					2.06	9.46												
65	14.70	15.0	0.524	5.00	34.50	120.99	8.69	26.74	26.74	26.74	26.74	26.74	26.74	26.74	26.74	26.74	26.74	26.74
66	14.70	15.0	0.524	5.00	35.98	127.87	9.23	29.45	29.45	26.93	26.93	26.93	26.93	26.93	26.93	26.93	26.93	26.93
67	14.70	13.0	0.524	5.00	34.90	122.79	9.64	28.71	28.71	27.75	27.75	27.75	27.75	27.75	27.75	27.75	27.75	27.75
68	14.70	13.0	0.524	5.00	36.27	129.18	10.05	27.13	27.13	28.64	28.64	28.64	28.64	28.64	28.64	28.64	28.64	28.64
69	14.54	13.0	0.524	5.00	35.98	127.12	10.05	27.13	27.13	28.05	28.05	28.05	28.05	28.05	28.05	28.05	28.05	28.05
70	14.98	12.0	0.524	5.00	35.53	125.00	9.62	28.00	28.00	29.05	29.05	29.05	29.05	29.05	29.05	29.05	29.05	29.05
71	14.97	12.0	0.524	5.00	33.65	112.67	9.62	28.00	28.00	26.84	26.84	26.84	26.84	26.84	26.84	26.84	26.84	26.84
72	14.98	12.0	0.524	5.00	34.38	119.69	9.62	28.00	28.00	27.76	27.76	27.76	27.76	27.76	27.76	27.76	27.76	27.76
73	14.95	12.0	0.524	5.00	37.69	135.33	9.62	29.81	29.81	27.67	27.67	27.67	27.67	27.67	27.67	27.67	27.67	27.67
74	14.91	11.0	0.524	5.00	34.72	121.44	9.62	27.04	27.04	28.52	28.52	28.52	28.52	28.52	28.52	28.52	28.52	28.52
75	14.91	11.0	0.524	5.00	34.72	121.44	9.62	27.04	27.04	28.52	28.52	28.52	28.52	28.52	28.52	28.52	28.52	28.52
76	14.91	15.0	0.524	5.00	34.68	122.16	9.62	29.45	29.45	27.93	27.93	27.93	27.93	27.93	27.93	27.93	27.93	27.93
Av					35.75	126.24	9.60	28.25	28.25	28.25	28.25	28.25	28.25	28.25	28.25	28.25	28.25	28.25
					1.12	5.90												
77	14.75	9.6	1.054	4.42	46.52	179.81	15.93	41.20	41.20	42.50	42.50	42.50	42.50	42.50	42.50	42.50	42.50	42.50
78	14.75	8.3	1.054	4.42	45.79	176.05	14.73	39.29	39.29	41.04	41.04	41.04	41.04	41.04	41.04	41.04	41.04	41.04
79	14.77	4.9	1.054	4.42	45.49	174.37	9.11	43.41	43.41	42.85	42.85	42.85	42.85	42.85	42.85	42.85	42.85	42.85
80	14.77	4.2	1.054	4.42	45.72	191.18	8.52	42.02	42.02	42.85	42.85	42.85	42.85	42.85	42.85	42.85	42.85	42.85
81	14.75	4.3	1.054	4.42	47.60	185.34	8.54	41.12	41.12	42.91	42.91	42.91	42.91	42.91	42.91	42.91	42.91	42.91
82	14.59	6.9	1.054	4.42	46.45	179.57	15.42	41.59	41.59	41.89	41.89	41.89	41.89	41.89	41.89	41.89	41.89	41.89
83	14.69	8.0	1.054	4.42	45.04	172.39	15.16	41.59	41.59	42.50	42.50	42.50	42.50	42.50	42.50	42.50	42.50	42.50
Av					46.52	179.81	12.50	41.20	41.20	42.50	42.50	42.50	42.50	42.50	42.50	42.50	42.50	42.50
					1.21	7.13												
84	14.95	8.0	1.053	4.03	52.41	242.35	14.55	46.23	46.23	45.49	45.49	45.49	45.49	45.49	45.49	45.49	45.49	45.49
85	14.95	3.6	1.053	4.03	59.34	246.42	16.59	41.22	41.22	41.95	41.95	41.95	41.95	41.95	41.95	41.95	41.95	41.95
86	14.93	9.9	1.053	4.03	59.37	246.69	17.25	43.63	43.63	49.28	49.28	49.28	49.28	49.28	49.28	49.28	49.28	49.28
87	14.96	14.0	1.053	4.03	59.57	249.31	16.89	46.82	46.82	46.70	46.70	46.70	46.70	46.70	46.70	46.70	46.70	46.70
88	14.84	15.0	1.053	4.03	60.82	240.77	16.73	46.82	46.82	46.70	46.70	46.70	46.70	46.70	46.70	46.70	46.70	46.70
89	14.84	5.8	1.053	4.03	60.39	253.99	16.25	45.39	45.39	48.00	48.00	48.00	48.00	48.00	48.00	48.00	48.00	48.00
90	14.84	5.3	1.053	4.03	60.05	252.09	16.25	45.39	45.39	48.00	48.00	48.00	48.00	48.00	48.00	48.00	48.00	48.00
91	14.84	15.6	1.053	4.03	59.05	246.49	16.25	45.39	45.39	48.00	48.00	48.00	48.00	48.00	48.00	48.00	48.00	48.00
Av					60.4	246.24	15.98	45.49	45.49	45.49	45.49	45.49	45.49	45.49	45.49	45.49	45.49	45.49
					1.79	4.36												

hd. No.	Ambient Pressure Tol	Ambient Temp °C	Charge Wt., V (lbs)	Sealed Distance R/W/3 1/3	Peak Pressure psi		Impulse of Noxious Phase in 10 msec/10						Duration of Noxious Phase in msec						Average Scaled Impulse		Average Scaled Duration								
					Side-On		Face-On		Pos. 1		Pos. 2		Pos. 3		Pos. 4		Side-On		Face-On		10 msec/10		1/3						
					Side-On	Face-On	Side-On	Face-On	Side-On	Face-On	Side-On	Face-On	Side-On	Face-On	Side-On	Face-On	Side-On	Face-On	Side-On	Face-On	Side-On	Face-On	Side-On	Face-On					
94	14.93	13.2	1,980	3.67	75.45	340.66	21.40	Lost	62.18	60.25	0.727	Lost	0.698	0.727	0.712	0.698	0.727	16.23	49.16	0.579	0.567	---	---	---	---	---	---		
95	14.92	13.6	1,980	3.67	74.41	338.58	21.40	Lost	64.90	59.53	0.727	Lost	0.698	0.727	0.712	0.698	0.727	---	---	---	---	---	---	---	---	---	---	---	
AV	---	---	---	---	---	---	---	---	---	---	---	---	---	---	---	---	---	---	---	---	---	---	---	---	---	---	---	---	
96	14.83	10.1	0,530	11.81	6.86	16.27	3.04	4.27	8.43	10.71	1.111	1.505	1.693	1.599	1.693	1.599	1.693	---	---	---	---	---	---	---	---	---	---	---	
97	14.93	9.8	0,530	11.81	7.12	16.99	3.04	4.55	5.36	11.43	1.111	1.709	1.997	1.824	1.997	1.824	1.997	---	---	---	---	---	---	---	---	---	---	---	
98	14.81	10.1	0,530	11.81	7.07	16.85	3.04	4.39	5.44	10.45	1.111	1.571	1.863	1.711	1.863	1.711	1.863	---	---	---	---	---	---	---	---	---	---	---	
99	14.61	9.8	0,530	11.81	7.06	16.81	3.04	4.77	5.73	11.34	1.111	1.648	1.948	1.795	1.948	1.795	1.948	---	---	---	---	---	---	---	---	---	---	---	
100	14.41	9.9	0,530	11.81	6.71	15.85	3.04	3.93	5.73	10.52	1.111	1.735	2.035	1.882	2.035	1.882	2.035	---	---	---	---	---	---	---	---	---	---	---	
101	14.21	9.9	0,530	11.81	6.95	16.51	3.04	3.50	5.30	10.75	1.111	1.735	2.035	1.882	2.035	1.882	2.035	---	---	---	---	---	---	---	---	---	---	---	
AV	---	---	---	---	---	---	---	---	---	---	---	---	---	---	---	---	---	---	---	---	---	---	---	---	---	---	---	---	
102	14.56	10.2	0,530	7.45	15.78	44.24	6.35	5.71	16.27	17.72	1.215	1.190	1.215	1.190	1.215	1.190	1.215	---	---	---	---	---	---	---	---	---	---	---	
103	14.58	12.2	0,520	7.45	15.48	43.19	6.35	6.38	17.07	20.41	1.215	1.190	1.215	1.190	1.215	1.190	1.215	---	---	---	---	---	---	---	---	---	---	---	
104	14.58	12.2	0,520	7.45	15.45	43.09	6.35	6.02	16.41	19.85	1.215	1.190	1.215	1.190	1.215	1.190	1.215	---	---	---	---	---	---	---	---	---	---	---	
105	14.58	12.0	0,520	7.45	15.20	42.21	6.35	6.29	17.36	20.94	1.215	1.190	1.215	1.190	1.215	1.190	1.215	---	---	---	---	---	---	---	---	---	---	---	
106	14.58	9.6	0,520	7.45	16.20	45.71	6.35	6.72	16.89	19.53	1.185	1.185	1.185	1.185	1.185	1.185	1.185	---	---	---	---	---	---	---	---	---	---	---	
107	14.58	9.6	0,520	7.45	15.53	43.35	6.35	6.02	15.35	18.16	1.185	1.185	1.185	1.185	1.185	1.185	1.185	---	---	---	---	---	---	---	---	---	---	---	
AV	---	---	---	---	---	---	---	---	---	---	---	---	---	---	---	---	---	---	---	---	---	---	---	---	---	---	---	---	
108	14.83	6.4	1,980	9.71	9.77	23.12	8.67	7.86	18.35	16.93	2.317	2.287	2.317	2.287	2.317	2.287	2.317	---	---	---	---	---	---	---	---	---	---	---	
109	14.83	6.2	1,980	9.71	9.77	22.49	8.67	8.79	17.49	17.31	2.317	2.317	2.317	2.317	2.317	2.317	2.317	---	---	---	---	---	---	---	---	---	---	---	
110	14.83	6.6	1,980	9.71	9.77	22.32	8.67	8.48	17.61	16.84	2.317	2.317	2.317	2.317	2.317	2.317	2.317	---	---	---	---	---	---	---	---	---	---	---	
111	14.83	6.9	1,980	9.71	9.77	22.97	8.67	7.99	18.68	18.34	2.317	2.317	2.317	2.317	2.317	2.317	2.317	---	---	---	---	---	---	---	---	---	---	---	
AV	---	---	---	---	---	---	---	---	---	---	---	---	---	---	---	---	---	---	---	---	---	---	---	---	---	---	---	---	
112	14.83	7.0	1,980	6.53	18.29	53.39	11.83	11.31	25.65	28.04	1.156	1.156	1.156	1.156	1.156	1.156	1.156	---	---	---	---	---	---	---	---	---	---	---	
113	14.83	7.5	1,980	6.53	18.71	54.56	11.83	11.95	29.35	27.66	1.156	1.156	1.156	1.156	1.156	1.156	1.156	---	---	---	---	---	---	---	---	---	---	---	
114	14.83	7.2	1,980	6.53	18.44	53.55	11.83	11.87	28.12	28.55	1.156	1.156	1.156	1.156	1.156	1.156	1.156	---	---	---	---	---	---	---	---	---	---	---	
115	14.75	7.6	1,980	6.53	18.99	55.64	11.83	11.87	28.12	27.41	1.156	1.156	1.156	1.156	1.156	1.156	1.156	---	---	---	---	---	---	---	---	---	---	---	
AV	---	---	---	---	---	---	---	---	---	---	---	---	---	---	---	---	---	---	---	---	---	---	---	---	---	---	---	---	---

Ra. No.	Ambient Pressure psia	Ambient Temp. °C	Charge Wt., W (lbs)	Scaled Distance R/W <sup>1/3</sup> ft/lb <sup>1/3</sup>	Peak Pressure psi		Impulse of Positive Phase in lb msec/in <sup>2</sup>				Duration of Positive Phase in msec				Average Scaled Impulse		Average Scaled Duration		
					Side-On	Face-On	Pos. 1	Pos. 2	Pos. 3	Pos. 4	Side-On	Pos. 1	Pos. 2	Pos. 3	Pos. 4	Side-On	Face-On	Side-On	Face-On
					psi		msec				msec				lb msec/in <sup>2</sup>		msec/lb <sup>1/3</sup>		
117	14.79	8.0	1.950	5.11	28.23	110.37	16.15	12.70	40.93	38.31	1.577	1.369	1.188	1.756	11.54	1.111			
118	14.79	8.0	1.950	5.11	28.23	110.37	15.38	12.31	37.99	35.35	1.422	1.223	1.282	1.794	11.54	1.111			
119	14.79	8.2	1.950	5.11	28.23	110.37	17.45	12.90	40.11	39.02	1.445	1.281	1.298	1.907	11.54	1.111			
120	14.79	8.2	1.950	5.11	28.23	110.37	15.36	12.51	37.92	35.90	1.382	1.201	1.294	1.714	11.54	1.111			
121	14.79	8.2	1.950	5.11	28.23	110.37	15.37	12.51	37.92	35.90	1.382	1.201	1.294	1.714	11.54	1.111			
AV							14.75		38.31		1.401		1.295		11.54	1.111			
122	14.72	9.3	1.980	4.11	68.09	298.76	17.06	10.92	49.70	47.20	1.092	1.092	1.074	1.074	15.15	1.084			
123	14.72	10.3	1.980	4.11	55.11	285.46	16.04	10.92	45.77	45.77	1.121	1.121	1.064	1.064	15.15	1.084			
124	14.72	10.2	1.980	4.11	57.19	286.86	15.10	10.92	45.04	45.04	1.128	1.128	1.064	1.064	15.15	1.084			
125	14.72	9.2	1.980	4.11	56.04	281.09	16.67	10.92	49.41	49.41	1.151	1.151	1.108	1.108	15.15	1.084			
126	14.61	8.0	1.980	4.11	69.75	309.22	16.67	10.92	59.72	59.72	1.151	1.151	1.108	1.108	15.15	1.084			
127	14.61	8.2	1.980	4.11	69.75	309.22	16.67	10.92	59.72	59.72	1.151	1.151	1.108	1.108	15.15	1.084			
AV							16.51		50.60		1.159		1.063		15.15	1.084			
128	14.61	10.3	1.980	3.22	128.14	549.79	20.27	7.22	68.51	68.22	0.684	0.684	0.587	0.510	15.15	1.084			
129	14.61	10.3	1.980	3.22	103.86	521.74	18.74	7.22	68.51	68.22	0.684	0.684	0.587	0.510	15.15	1.084			
130	14.61	10.3	1.980	3.22	112.98	528.90	18.74	7.22	68.51	68.22	0.684	0.684	0.587	0.510	15.15	1.084			
131	14.78	7.8	1.980	3.22	105.23	528.90	20.27	7.22	77.99	71.32	0.547	0.774	0.658	0.601	15.15	1.084			
132	14.78	8.0	1.980	3.22	115.98	599.80	20.27	7.22	77.99	71.32	0.547	0.774	0.658	0.601	15.15	1.084			
133	14.78	8.4	1.980	3.22	115.98	599.80	20.27	7.22	77.99	71.32	0.547	0.774	0.658	0.601	15.15	1.084			
AV							20.27		71.22		0.684		0.592		15.15	1.084			
134	14.63	8.5	1.980	2.52	170.95	980.05	22.04	14.46	103.0	103.0	0.667	0.667	0.414	0.414	15.15	1.084			
135	14.71	11.1	1.980	2.52	167.07	954.31	17.37	14.46	90.96	78.93	0.481	0.481	0.408	0.375	15.15	1.084			
136	14.91	10.0	1.980	2.52	172.24	987.97	16.83	14.46	90.96	78.93	0.481	0.481	0.408	0.375	15.15	1.084			
137	14.82	10.9	1.980	2.52	163.66	962.35	16.83	14.46	90.96	78.93	0.481	0.481	0.408	0.375	15.15	1.084			
138	14.82	10.9	1.980	2.52	163.66	962.35	16.83	14.46	90.96	78.93	0.481	0.481	0.408	0.375	15.15	1.084			
139	14.82	10.9	1.980	2.52	167.14	984.26	16.52	14.46	90.96	78.93	0.481	0.481	0.408	0.375	15.15	1.084			
140	14.62	10.2	1.980	2.52	166.13	968.36	18.43	14.46	90.96	78.93	0.481	0.481	0.408	0.375	15.15	1.084			
AV							18.55		91.30		0.621		0.411		15.15	1.084			
141	14.66	10.5	1.980	1.51	454.23	3380.7	17.97	23.82	130.5	130.5	0.299	0.299	0.232	0.244	15.15	1.084			
142	14.83	10.8	1.980	1.51	476.49	3521.1	21.92	23.82	130.5	130.5	0.299	0.299	0.232	0.244	15.15	1.084			
AV							21.26		149.9		0.299		0.238		15.15	1.084			









DISTRIBUTION LIST

<u>No. of Copies</u>	<u>Organization</u>	<u>No. of Copies</u>	<u>Organization</u>
4	Chief of Ordnance Department of the Army Washington 25, D. C. Attn: ORDTB - Tol Sec ORDTA ORDTU ORDTX-AR	8	Chief, Bureau of Aeronautics Department of the Navy Washington 25, D. C. Attn: Armament Div. 2 cys Research Div. 1 cy Design Elements Div. 1 cy Evaluation Div. 1 cy Military Requirements Div. 1 cy Aircraft Div. 1 cy
10	British Joint Services Mission 1800 K Street, N. W. Washington 6, D. C. Attn: Mr. John Izzard, Reports Officer Of Interest to: Mr. G. Simm, R.A.E.	1	Chief of Naval Operations Dept. of the Navy Washington 25, D. C. Attn: Op 574 - Dr. J. Steinhardt
4	Canadian Army Staff 2450 Massachusetts Ave., N. W. Washington 8, D. C.	1	Naval Ordnance Laboratory Corona, California Attn: Dr. H. A. Thomas
3	Chief, Bureau of Ordnance Department of the Navy Washington 25, D. C. Attn: ReO	5	Chief of Staff U. S. Air Force Washington 25, D. C. Attn: AFDRD-AC - 2 cys DCS/O - Operations Analysis Div. AFDRQ
2	Commander Naval Proving Ground Dahlgren, Virginia	2	Director Air University Maxwell Air Force Base, Ala. Attn: Air Univ. Lib.
2	Commander Naval Ordnance Lab. White Oak Silver Spring 19, Md.	1	Director of Research and Development U. S. Air Force Washington 25, D. C. Attn: Armament Div. (AFDRD- AR/1)
1	Commander Naval Air Development Center Johnstown, Pennsylvania	3	Commander Wright Air Dev. Center Wright-Patterson Air Force Base, Ohio Attn: WCLGR-4 1 cy WCLDI 1 cy WCLSS-1 1 cy
1	Superintendent Naval Postgraduate School Monterey, California		

DISTRIBUTION LIST

<u>No. of Copies</u>	<u>Organization</u>	<u>No. of Copies</u>	<u>Organization</u>
1	Aerojet-General Corporation 6352 North Irwindale Road Azusa, California	1	University of Pittsburgh Pittsburgh, Pennsylvania Attn: Dr. Malin
1	Cornell Aeronautical Lab., Inc. 4455 Genessee Street Buffalo 21, New York	1	University of Chicago Institute for Air Weapons Research Museum of Science and Industry Chicago 37, Illinois Attn: Dr. David Saxton Mr. Herbert Hesse
1	Denver Research Institute University of Denver Denver 10, Colorado	1	Office Asst. Secretary of Defense (R&D) Committee on Ordnance Washington 25, D. C.
1	General Electric Company Aircraft Products Division 600 Main Street Johnson City, New York	1	Commander Air Proving Ground Command Eglin Air Force Base, Florida Attn: Director of Armament
1	General Electric Company Aeronautics and Ordnance Systems Division Schenectady 5, New York Attn: H. C. Page	1	
1	Institute for Cooperative Research Project THOR 3506 Greenway Baltimore 18, Maryland		
1	Massachusetts Institute of Technology Building 23-111 Cambridge 39, Massachusetts Attn: Dr. James Mar		
1	Massachusetts Institute of Technology Room 41-219 Cambridge 39, Massachusetts Attn: Dr. Emmett A. Pitner		